WATER RESEARCH 53 (2014) 35–46

Available online at www.sciencedirect.com

ScienceDirect

journal homepage: www.elsevier.com/locate/watres

Adhesion of bacterial pathogens to soil colloidal particles: Influences of cell type, natural organic matter, and solution chemistry

Wenqiang Zhao [a], Sharon L. Walker [b], Qiaoyun Huang [a], Peng Cai [a,*]

[a] State Key Laboratory of Agricultural Microbiology, College of Resources and Environment, Huazhong Agricultural University, Wuhan 430070, China

[b] Department of Chemical and Environmental Engineering, University of California, Riverside, CA 92521, USA

ARTICLE INFO

Article history:
Received 3 September 2013
Received in revised form
20 November 2013
Accepted 5 January 2014
Available online 16 January 2014

Keywords:
Pathogen
Adhesion
Soil colloid
Solution chemistry
DLVO theory

ABSTRACT

Bacterial adhesion to granular soil particles is well studied; however, pathogen interactions with naturally occurring colloidal particles (<2 μm) in soil has not been investigated. This study was developed to identify the interaction mechanisms between model bacterial pathogens and soil colloids as a function of cell type, natural organic matter (NOM), and solution chemistry. Specifically, batch adhesion experiments were conducted using NOM-present, NOM-stripped soil colloids, *Streptococcus suis* SC05 and *Escherichia coli* WH09 over a wide range of solution pH (4.0–9.0) and ionic strength (IS, 1–100 mM KCl). Cell characterization techniques, Freundlich isotherm, and Derjaguin–Landau–Verwey–Overbeek (DLVO) theory (sphere–sphere model) were utilized to quantitatively determine the interactions between cells and colloids. The adhesion coefficients (K_f) of *S. suis* SC05 to NOM-present and NOM-stripped soil colloids were significantly higher than *E. coli* WH09, respectively. Similarly, K_f values of *S. suis* SC05 and *E. coli* WH09 adhesion to NOM-stripped soil colloids were greater than those colloids with NOM-present, respectively, suggesting NOM inhibits bacterial adhesion. Cell adhesion to soil colloids declined with increasing pH and enhanced with rising IS (1–50 mM). Interaction energy calculations indicate these adhesion trends can be explained by DLVO-type forces, with *S. suis* SC05 and *E. coli* WH09 being weakly adhered in shallow secondary energy minima via polymer bridging and charge heterogeneity. *S. suis* SC05 adhesion decreased at higher IS 100 mM, which is attributed to the change of hydrophobic effect and steric repulsion resulted from the greater presence of extracellular polymeric substances (EPS) on *S. suis* SC05 surface as compared to *E. coli* WH09. Hence, pathogen adhesion to the colloidal material is determined by a combination of DLVO, charge heterogeneity, hydrophobic and polymer interactions as a function of solution chemistry.

1. Introduction

The United States and China annually produce 317 × 10^6 and 300 × 10^7 tons of animal manure, respectively (Browner et al., 2001; Huang et al., 2008); whereas, the production is approximately 10^{10}–10^{11} tons worldwide (Pachepsky et al., 2006). Over the past decades, large amounts of fecal wastes have been applied to the soil as a source of plant nutrients. Meanwhile, these wastes may contain various pathogenic microorganisms

* *Corresponding author*. Tel.: +86 27 87671033; fax: +86 27 87280670.
E-mail address: cp@mail.hzau.edu.cn (P. Cai).

0043-1354/$ – see front matter © 2014 Elsevier Ltd. All rights reserved.
http://dx.doi.org/10.1016/j.watres.2014.01.009

if not managed properly (Tyrrel and Quinton, 2003; Cotruvo et al., 2004). Application of solid wastes to soil introduces high concentrations of pathogens associated with human diseases (Santamaria and Toranzos, 2003; Haznedaroglu et al., 2009). For instance, *Streptococci* and fecal coliforms have been widely detected in animal manures and soil environments by genetic techniques (Unc and Goss, 2004). During the summer of 2005 in China, a large outbreak of acute diseases linked to *Streptococcus suis* appeared suddenly, which was ascribed to close contact with pig wastes or ingestion of contaminated food (Gottschalk et al., 2010). The Beijing Centers for Disease Control and Prevention reported that 205 people were infected, with a mortality rate of nearly 20%. A case of male farmer infection was also reported in the United States in 2006 (Gottschalk et al., 2007). Another bacterial pathogen of concern is *Escherichia coli* (referred to as an indicator of fecal contamination), from which outbreaks linked to contaminated vegetables, soil or groundwater have led to serious diseases (Cai et al., 2013). It was reported that pathogenic *E. coli* causes ~73,000 illnesses, ~2200 hospitalizations, and ~61 deaths annually in the United States (Wang et al., 2011). Pathogens presence, through their retention in the upper layers of soil or surface runoff, may pose a risk to human and livestock health (Dhand et al., 2009). Therefore, a thorough understanding of pathogen adhesion to soil components is of great importance for assessing the fate of pathogens in soil and aquatic environments.

Generally, a two-step mechanism mediates bacterial adhesion to solid surfaces (Zita and Hermansson, 1994). The first step is governed by long-range physiochemical interactions such as Lifshitz–van der Waals and electrostatic forces that described by the Derjaguin–Landau–Verwey–Overbeek (DLVO) theory (Bakker et al., 2004), as well as bridging effects among the organic matter or polymers that exist on collector surfaces (Parent and Velegol, 2004). These forces determine whether the cells are able to get close enough to solid surfaces such that adhesion can occur. The second step involves short-range irreversible adhesion by forming hydrophobic force, hydrogen bonding, or steric interaction (Gordesli and Abu-Lail, 2012). Both steps are affected by the surface properties of the interacting surface and electrolytic environment. The investigated factors include bacterial strain (Li and Logan, 2004; Morrow et al., 2005), mineral type (Salerno et al., 2004; Rong et al., 2008), solution chemistry (Yee et al., 2000; Farahat et al., 2010), cell surface features (e.g., proteins and polysaccharides) (Walker et al., 2005a; Shephard et al., 2010), and organic matter (Parent and Velegol, 2004; Foppen et al., 2008; Park and Kim, 2009). The organic matter (e.g., humic acid) used in previous cell adhesion studies was usually purchased from a company and had been modified (Parent and Velegol, 2004; Foppen et al., 2008; Park and Kim, 2009), which differs from the real heterogenous state of natural organic matter (NOM) in the soil. Additionally, most previous work examined the impacts of various physical, chemical, and biological factors on cell adhesion to granular and flat mineral surfaces, far less attention has been directed towards the natural colloidal soil particles. Extrapolating the adhesion mechanisms in pure minerals to those in soil particles is more complicated because of the higher complexity of the latter consisting of NOM and multiple mineral types (Brady, 1990). Moreover, it should be noted that pathogen adhesion to soil particle surfaces (soil colloids <2 μm in size for this study) has not been systematically explored across a wide range of ionic strength (IS) and solution pH.

After pathogens were introduced through the application of biosolids in soil, they can be trapped in soil pores or adhered by soil particles, fragments of vegetation, and manure particles (Tyrrel and Quinton, 2003; Pachepsky et al., 2006). Once suspended in water during the rainfall and irrigation events, bacteria may also be transported with surface or subsurface water flow as free or adhered cells via association with soil particles (Pachepsky et al., 2006; Guber et al., 2007). Recently, a small number of studies have shown that soil colloids played an important role in bacterial adhesion. For example, Oliver et al. (2007) found that most of the *E. coli* cells (65%) were associated with soil particulates <2 μm in diameter. For the 2–3 μm, 4–15 μm, 16–30 μm, and ≥31 μm size fractions, the percentages of adhered cells were 7, 14, 12, and 2% respectively. Guber et al. (2007) observed that in the absence of manure colloids, fecal coliforms adhesion to soil silt (2–50 μm) and clay particles (<2 μm) was much higher than those to sand particles (62.5–500 μm). Soupir et al. (2010) found that more than 60% of adhered *E. coli* and enterococci were associated with fine-size particles (8–62 μm). The lowest *E. coli* concentration in runoff occurred from the silty loam soils, which have higher clay and organic contents. Wu et al. (2011) reported that the maximum number of *Pseudomonas putida* cells that adhered to the clay fraction of Red soil (Ultisol) was 4 and 62 times as great as that by silt and sand fractions, respectively. Despite these initial efforts, few studies have given sufficient explanation with regard to bacterial adhesion to colloidal particles. Information on the comprehensive surface properties of pathogens and soil colloids under varying solution parameters is lacking. To the best of our knowledge, the interaction forces between pathogens and natural soil particles have never been investigated.

The objectives of the present work were to elucidate how pathogens (*S. suis* SC05 and *E. coli* WH09) adhesion to soil colloids respond to the changes in cell type, NOM, and solution chemistry. Surface physico-chemical properties of the bacteria and soil colloids were extensively characterized over a wide range of pH (4.0–9.0) and ionic strength (IS, 1–100 mM). These solution values encompass most soil environmental relevant conditions. Furthermore, the DLVO theory (sphere–sphere model) was firstly utilized to predict energy profiles and provide insight into the interaction mechanisms of pathogen-soil colloid systems.

2. Materials and methods

2.1. Bacterial growth and preparation

Gram-negative *E. coli* WH09 and Gram-positive *S. suis* SC05, obtained from the State Key Laboratory of Agricultural Microbiology, were isolated from soils around a pig farm in Wuhan, Hubei Province, China. Bacterial growth and preparation methods are provided in the Supplementary data.

2.2. Bacterial cell characterization

The zeta potential and hydrodynamic diameter of bacteria were determined by Zetasizer (Nano ZS90, Malvern

Instruments Ltd., UK). The electrophoretic mobilities of *E. coli* WH09 and *S. suis* SC05 cells were evaluated at different pH (4.0–9.0) and IS (1–100 mM KCl). Zeta potential was calculated from electrophoretic mobility according to the Smoluchowski equation (Hiemenz, 1977). All measurements were conducted at 25 °C and repeated three times using freshly rinsed cells (10^7 to 10^8 cells per mL).

Cell surface hydrophobicity was measured by the microbial adhesion to hydrocarbon (MATH) test (Parent and Velegol, 2004; Tazehkand et al., 2008). Briefly, 1 mL of *n*-dodecane (laboratory grade) was added to 4 mL of cell suspension (OD_{600} ~0.2) in 15 mL test tube (diameter, 1.7 cm; length, 11.8 cm). The mixture was vortexed at full speed for 2 min and then left to stand for 45 min to allow sufficiently phase separation. The hydrophobicity of each cell type was quantified as the percentage of total cells partitioned into the hydrocarbon phase. The mean percentage of hydrophobicity was calculated using triplicate samples at different pH (4.0–9.0) and IS (1–100 mM KCl).

Potentiometric titrations of bacteria were performed using an automatic potentiometric titrator (Metrohm titrator 836, Metrohm, Switzerland) under a N_2 atmosphere at 25 °C. Bacterial suspensions with concentrations of 6.0×10^8 cells per mL in 10 mM KCl were titrated using 0.0916 M HCl and 0.0911 M KOH solutions. The surface charge density was calculated from the amount of base consumed by suspended cells during the titration between pH 2.5 and pH 10.0, accounting for the cell surface area (Chen and Walker, 2007).

The extracellular polymeric substances (EPS) content and composition were analyzed. Total EPS, sugar, and protein contents were assayed by ethanol precipitation (Kim and Walker, 2009), phenol-sulfuric acid, and bicinchoninic acid method (Boisynthesis Co., Ltd., Beijing), respectively (Cao et al., 2011). The specific surface area (SSA) of bacteria was measured via the methylene blue adsorption method (He and Tebo, 1998).

2.3. *Soil colloidal particles*

Brown soil (Alfisol) was sampled from the 0–20 cm layer of a farmland in Tianwai Village, Taishan, Shandong Province, China. After removing the organic residues, the soil was rinsed in distilled-deionized water (ddH_2O) and dispersed by adding 0.01 M NaOH solution dropwise to pH 7.5 together with sonication (Xiong, 1985). The <2 μm colloidal fraction of the soil was separated by sedimentation (Xiong, 1985). This colloidal sample was the natural organic matter (NOM)-present fraction. To obtain NOM-stripped fraction, the colloidal suspension was treated by H_2O_2 to oxidize organic matter (Cai et al., 2006). After flocculation by adding $CaCl_2$ solution, the colloidal suspension was washed with ddH_2O and ethanol to be free of Cl^- (centrifuged at 3220 × *g* for 20 min), and then air-dried. 81.1% of organic matter (by mass) was removed using the oxidization method (Table 1). In this study, there still remained 18.9% of organic matter in NOM-stripped colloids. Thus, the comparison of cell adhesion to NOM-present soil colloid with that to NOM-stripped fraction may only reflect the effect of most NOM in soil colloids on bacterial adhesion behavior.

Table 1 – Measured surface properties of *S. suis* SC05, *E. coli* WH09, NOM-present and NOM-stripped soil colloids.

Pathogen/Soil type	Radius (μm)	SSA[a] ($m^2\ g^{-1}$)	ZP[b] (mV)	PATH[c] (%)	CEC[d] ($cmol\ kg^{-1}$)	NOM[e] ($g\ kg^{-1}$)	EPS[f] ($\mu g/10^8$ cells)	Sugar (μg/10 cells)	Protein ($\mu g/10^8$ cells)	Surface charge density[g] ($\mu C/cm^2$)
S. suis SC05	0.34 ± 0.04	109.1	−28.9 ± 1.8	7.9 ± 2.9	–	–	54.67 ± 3.50	12.78 ± 0.15	28.70 ± 0.19	213.0 ± 3.9
E. coli WH09	0.44 ± 0.05	39.0	−38.9 ± 1.7	15.5 ± 1.9	–	–	26.25 ± 2.32	11.73 ± 0.13	4.80 ± 0.04	541.1 ± 14.4
NOM-present colloid	0.61 ± 0.02	83.8	−27.1 ± 1.1	58.6 ± 4.8	63.1	10.6	–	–	–	891.1 ± 12.0
NOM-stripped colloid	0.43 ± 0.01	101.6	−23.0 ± 1.4	51.4 ± 4.1	55.8	2.0	–	–	–	722.2 ± 6.4

[a] SSA is specific surface area.
[b] ZP is zeta potential.
[c] PATH indicates the relative hydrophobicity as the percentage of particle partitioned in *n*-dodecane.
[d] CEC is cation-exchange capacity.
[e] NOM is natural organic matter.
[f] EPS is extracellular polymeric substances.
[g] The value was calculated from the amount of base consumed by suspended cells during the titration between pH 2.5 and pH 10.0, accounting for the cell surface area. Zeta potential and hydrophobicity values were measured at pH 6.0 and IS 1 mM.

The mineral fraction of the colloidal particle was kaolinite (5%), hydromica (21%) and vermiculite (74%), which was determined by X-ray diffraction (XRD) using monochromated Fe Kα radiation (Cai et al., 2006). The zeta potential, diameter, hydrophobicity, NOM content, cation-exchange capacity (CEC), and SSA of soil colloids were analyzed by Zetasizer (Nano ZS90, Malvern Instruments Ltd., UK), particle adhesion to hydrocarbon (PATH) test (Parent and Velegol, 2004; Tazehkand et al., 2008), $K_2Cr_2O_7$ digestion, $NH_4C_2H_3O_2$ displacement (Fagbenro and Agboola, 1999), and N_2 adsorption method (Autosorb-1, Quantachrome Instruments, USA), respectively. The relative acidity and surface charge density were also obtained by automatic potentiometric titrator (Metrohm titrator 836, Metrohm, Switzerland). Properties of the soil colloids are listed in Table 1.

2.4. Adhesion experiments

The isothermal adhesion curve of bacteria to colloidal particles was performed in 1 mM KCl solution at pH 6.0 (close to the pH of Brown soil, pH 5.9). One hundred mg of colloidal particles was mixed with 30 mL of bacterial solutions (0, 0.6×10^{10}, 1.2×10^{10}, 1.8×10^{10}, 2.4×10^{10}, 3.0×10^{10}, 3.6×10^{10}, and 4.2×10^{10} cells of *S. suis* SC05 or *E. coli* WH09). The mixture was shaken at 150 rev min^{-1} and 25 °C for 1 h (sufficient for the reaction to reach a plateau). The un-adhered bacteria were separated from those adhered to colloidal particles by injecting 5 mL of sucrose solution (60% by weight) (Rong et al., 2008). Sucrose can create a density gradient in adhesion mixture. The suspension was centrifuged at 3220 × *g* for 20 min, and then the soil colloid-cell aggregates sank to the bottom of the tubes. Preliminary experiments indicated that the sucrose solution does not significantly affect the number of bacteria determined (Rong et al., 2008). The un-adhered cells in the supernatant were determined by total protein analysis (details on the method are shown in the Supplementary data (Bradford, 1976). The number of adhered bacteria (10^{10} cells per dry weight of soil colloid) was calculated as the difference between the number added and the number recovered in the supernatant. The adhesion experiments were also conducted in the presence of 1, 5, 10, 50, and 100 mM of KCl (unadjusted pH of 5.6–5.8), wherein 2.1×10^{10} bacterial cells and 100 mg of soil particles were employed. Similar experiments were carried out at pH ranging from 4.0 to 9.0 (IS 1 mM KCl). Cell concentration was enumerated based upon protein content. Figures regarding the calibration curves between the pathogen concentration and protein content are presented in Fig. S1 of the Supplementary data.

2.5. Calculation of interaction energy profiles

The classic DLVO theory was applied to predict the interaction energies between the pathogens and soil colloids as a function of separation distance and solution chemistry (Hogg et al., 1966; Gregory, 1981; Kim et al., 2010; Syngouna and Chrysikopoulos, 2010). Zeta potential (in place of surface potential) and radius values were utilized in sphere–sphere model. Calculation details are given in the Supplementary data.

2.6. Statistics

All adhesion experiments were performed in triplicate. The data are presented as the mean ± standard deviation of the mean (x ± SDM). When not indicated, the SDMs were within the dimensions of the symbols. Statistical differences between mean values were analyzed using a Student's *t* test. Spearman correlation and linear regression analysis were performed using SPSS 17.0 for Windows (SPSS Inc, Chicago, Illinois, USA). *P* values greater than or equal to 0.05 suggest that the differences are not statistically significant within a 95% confidence interval.

3. Results and discussion

3.1. Surface characteristics of bacteria and soil colloids

Zeta potential reflects the net charge on bacterial or soil colloidal surface (Kirby and Hasselbrink, 2004), and the values measured for these surfaces are reported in Fig. 1a across the range of pH from 4.0 to 9.0. All of the particles (cell and soil) were negatively charged and the magnitude of this charge

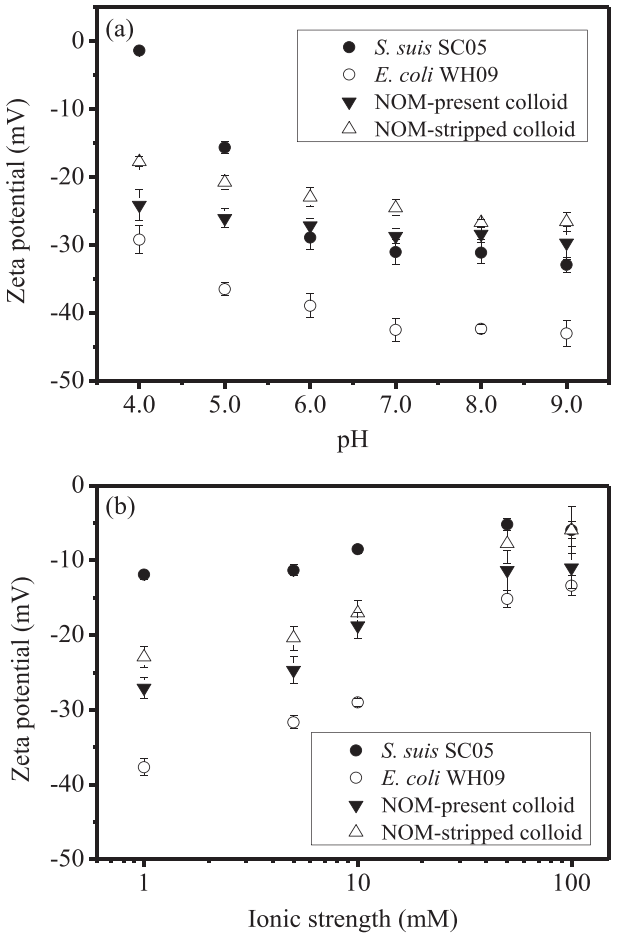

Fig. 1 – Zeta potential of *S. suis* SC05, *E. coli* WH09, NOM-present and NOM-stripped soil colloids as a function of (a) pH (at 1 mM KCl) and (b) IS (at unadjusted pH of 5.6–5.8). Error bars are the standard deviation of three replicates.

increased with pH, which is ascribed to the deprotonation of surface functional groups with the addition of base (Schinner et al., 2010). Fig. 1b displays data for changing IS, from which it can be observed the zeta potentials of bacteria and soil colloids were less negative with the increase of IS (1–10 mM). The reduction in zeta potential is attributed to the charge screening by counter ions and double layer compression outside the surfaces of the cells and soil colloids (Walker et al., 2004). However, the zeta potentials of the cells and soil colloids remained constant at higher IS from 50 to 100 mM ($P > 0.05$), which indicates a limit to the compression of the double layer (Sharma et al., 1985). *S. suis* SC05 cells were less negatively charged than *E. coli* WH09 across the range of pH and IS conditions. Surface charges on NOM-stripped colloids were less negative than those of NOM-present colloids under all the experimental conditions, probably due to the removal of negatively charged organic matter (e.g., humic and fulvic acids) from the soil colloids (Amirbahman and Olson, 1993). The previously reported zeta potentials of soil mineral samples showed more variation than our current soil colloids. The zeta potentials of soil colloids were in the range of −17.7 mV to −29.7 mV and −27.1 mV to −6.0 mV at varied pH (4.0–9.0) and IS (1–100 mM), respectively. However, the zeta potentials of corundum, hematite, quartz, and kaolinite declined quite markedly from about +20 mV to −110 mV with increasing pH (4.0–9.0) (Deo et al., 2001; Zhao et al., 2012). At 1–100 mM, the zeta potentials of quartz sand and pyrophyllite also changed strongly, with values ranging from −48 mV to −2 mV (Morrow et al., 2005; Haznedaroglu et al., 2009). The relative low variation of zeta potentials of soil colloids possibly resulted from the balance of kaolinite (variable-charge mineral), hydromica, vermiculite (permanent-charge mineral) and NOM in soil colloids that exhibited different charge sensitivities to solution chemistry.

The effects of pH and IS on the bacterial and soil colloids hydrophobicity are presented in Fig. 2a and b, respectively. No significant changes in the hydrophobicity of *E. coli* WH09 (16.2% ± 1.1%) were observed at pH 4.0–9.0 and of *S. suis* SC05 (7.5% ± 0.3%) at pH 4.0–6.0 ($P > 0.05$) (Fig. 2a). *S. suis* SC05 exhibited greater sensitivity to solution chemistry. Notably, the hydrophobicity of *S. suis* SC05 at pH 7.0–9.0 increased dramatically compared with those at pH 4.0–6.0, which was ascribed to the greater structural transitions of cell surface molecules at alkaline conditions causing more hydrophobic sites to be exposed (Alizadeh-Pasdar and Li-Chan, 2000). *E. coli* WH09 was more hydrophobic than *S. suis* SC05 except at pH 9.0. In the IS range of 1–10 mM, the hydrophobicity values of both bacterial strains were 31.1% ± 0.2% (Fig. 2b). The general features of cell hydrophobicity maintained the same at low IS, whereas the hydrophobicity decreased by 3.2% (*E. coli* WH09) to 9.0% (*S. suis* SC05) at high IS ranging from 50 to 100 mM. A similar decreasing trend for *E. coli* WH09 was reported previously (Haznedaroglu et al., 2009). Cell surface polymers were compressed at high IS and likely contributed to the decrease in the exposure of hydrophobic functional groups outside the cell surface (Alizadeh-Pasdar and Li-Chan, 2000; Abu-Lail and Camesano, 2003). These above bacterial hydrophobicity values were comparable to those of other strains (16.7–68.3%) (Haznedaroglu et al., 2008, 2009). The hydrophobicity of a soil particle, unlike that of a bacterial cell, was independent of pH

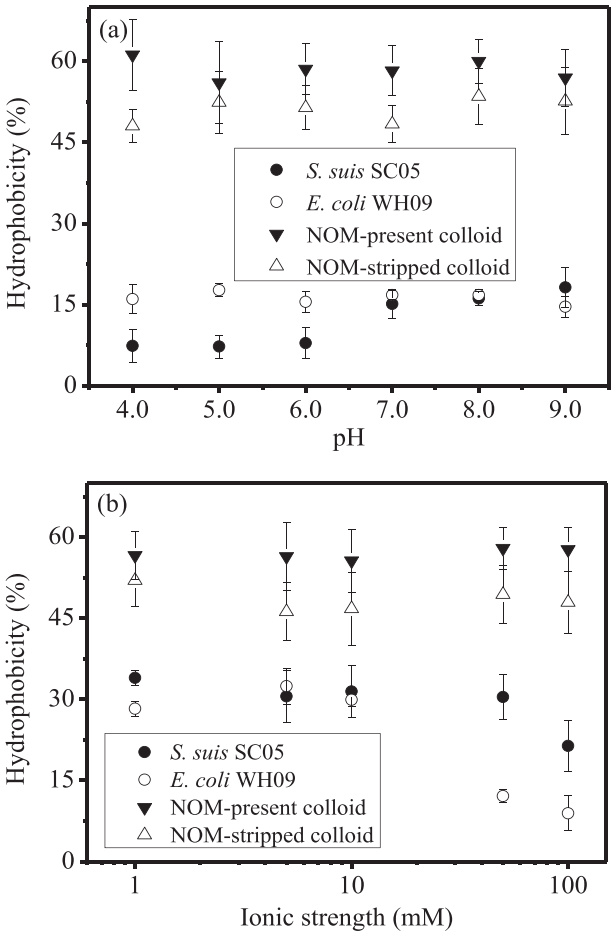

Fig. 2 – Hydrophobicity of *S. suis* SC05, *E. coli* WH09, NOM-present and NOM-stripped soil colloids as a function of (a) pH (at 1 mM KCl) and (b) IS (at unadjusted pH of 5.6–5.8). Error bars are the standard deviation of three replicates.

and IS (Wang et al., 2011) and remained constant (46.2–61.2%, $P > 0.05$) under all conditions. In Fig. 2a and b, the hydrophobicity of NOM-present colloid (57.7%) was on average larger than that of NOM-stripped colloid (49.7%) under different solution chemistry. The NOM fraction contributed slightly (8.0%) to the overall hydrophobicity of the soil colloid. To the best of our knowledge, the influence of solution chemistry parameters on soil colloidal hydrophobicity has not been studied before. The hydrophobicity of soil colloids were completely different from clay minerals (kaolinite, montmorillonite), which displayed a large range of hydrophobicity (5%–95%) and irregular variation with the change of solution conditions (pH 3.0–10.0; $MgCl_2$ 10–500 mM) (Hong et al., 2013).

As shown in Table 1, the total EPS content of *S. suis* SC05 (54.67 ± 3.50 μg/10^8 cells) was higher than that of *E. coli* WH09 (26.25 ± 2.32 μg/10^8 cells) ($P < 0.05$). EPS has been credited with contributing to the overall heterogeneity of bacterial surfaces (Omoike and Chorover, 2004; Walker et al., 2005a). Thus, *S. suis* SC05 cellular structures exhibited greater heterogeneity and non-uniformity in the distribution of the exposed functional groups and surface charges (Elimelech et al., 2000). The sugar content of *S. suis* SC05 (12.78 ± 0.15 μg/10^8 cells) was

comparable to that of *E. coli* WH09 (11.73 ± 0.13 μg/10^8 cells), while *S. suis* SC05 protein content (28.70 ± 0.19 μg/10^8 cells) was much greater than *E. coli* WH09 (4.80 ± 0.04 μg/10^8 cells). The outer membrane proteins of bacteria are mostly hydrophilic, which decreases surface hydrophobicity (Nikaido, 2003). The trends from the hydrophobicity analysis that *S. suis* SC05 had lower values and higher sensitivity were corroborated by the more protein content of *S. suis* SC05 cell. Further evidence of the sensitivity of cell hydrophobicity to proteins can be found in the literature (Alizadeh-Pasdar and Li-Chan, 2000; Bruinsma et al., 2001; Walker et al., 2005b).

Potentiometric titration was used to measure the charge distribution across the particle surface. The surface charge density of *E. coli* WH09 (541.1 μC/cm^2) was almost 2.5 times as high as that of *S. suis* SC05 (213.0 μC/cm^2), while that of NOM-present colloid (891.1 μC/cm^2) was greater than NOM-stripped colloid (722.2 μC/cm^2). Thus, compared to *S. suis* SC05 and NOM-stripped colloid, more dissociable functional groups are present on *E. coli* WH09 and NOM-present colloid surface, respectively.

3.2. *Effects of cell strain and NOM on pathogen adhesion*

The equilibrium adhesion isotherms of *S. suis* SC05 and *E. coli* WH09 to NOM-present and NOM-stripped colloids at pH 6.0 and 1 mM KCl are shown in Fig. 3. The number of adhered bacteria increased with the initial cell concentrations. The adhesion data conformed to the Freundlich equation: $C_s = K_f \cdot C^{1/n}$, where C_s is the number of pathogens adhered per unit mass of soil colloids (10^{10} cells g^{-1}), K_f is the coefficient related to adhesion capacity (mL g^{-1}), C is the pathogen concentration in equilibrium solution (10^{10} cells mL^{-1}), and $1/n$ stands for the linearity exponent. As presented in Table 2, the Freundlich equation described the adhesion reasonably well, with R^2 (coefficient of determination) ranging from 0.971 to 0.993 for each system investigated. The K_f values of *S. suis* SC05 adhesion to soil colloids were 4.1–8.1 times as large as those of *E. coli* WH09. Pathogens adhesion to NOM-stripped colloid (210.6–856.1 mL g^{-1}) was far greater than those to NOM-present colloid (31.3–252.6 mL g^{-1}), which suggests NOM inhibits cell adhesion to soil colloids.

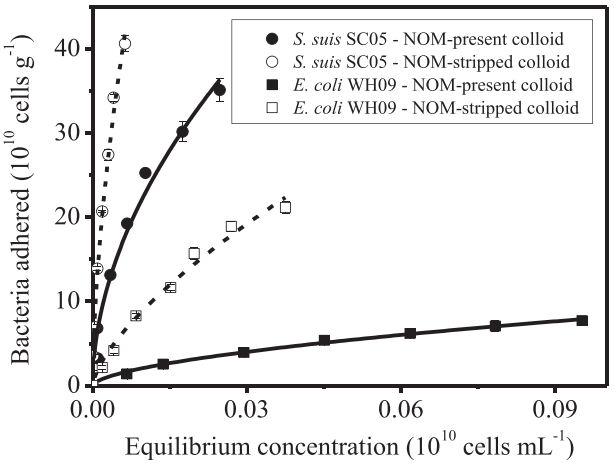

Fig. 3 – Equilibrium adhesion isotherms of *S. suis* SC05 and *E. coli* WH09 to soil colloids at pH 6.0 and 1 mM KCl. The solid and dashed lines represent fitted curves of Freundlich equations for NOM-present and NOM-stripped colloids, respectively. Error bars are the standard deviation of three replicates.

The surface physicochemical properties of bacteria and soil particles were used to clarify the interaction mechanisms between them (Walker et al., 2005a; Haznedaroglu et al., 2008). At pH 6.0, the net surface charges of pathogens and soil colloids were all negative, yielding electrostatic repulsive forces (Table 1). More negative charges (absolute value of zeta potential) result in stronger repulsive interactions. The surface charges of *E. coli* WH09 cells were more negative and less heterogenous than *S. suis* SC05, which produced larger repulsive forces between *E. coli* WH09 and the soil colloids. The more surface charge density existing on *E. coli* WH09 surface also increases the degree of repulsions (Walker et al., 2005b). Similarly, the CEC and absolute zeta potentials of NOM-present colloid were larger than those of NOM-stripped colloid. More negative charges on the NOM-present colloid surface were responsible for its smaller K_f values. The above results indicate that electrostatic interaction plays an important role in adhesion. The hydrophobicity of *E. coli* WH09 (15.5%) and NOM-present colloid (58.6%) were higher than those of *S. suis* SC05 (7.9%) and NOM-stripped colloid (51.4%), respectively (Table 1). These data did not agree with their K_f values, which suggest that hydrophobic effect is not the main mechanism controlling pathogen adhesion. It was also observed that *E. coli* WH09 deposition in flow systems were not significantly correlated ($P > 0.05$) with hydrophobicity values as in previous studies (Li and Logan, 2004; Kim and Walker, 2009).

The DLVO theory was used to provide greater insight into the bacterial adhesion trends (Vigeant et al., 2002). This theory considers the sum of van der Waals and electrostatic interactions. Positive interaction energy indicates a repulsive force between the bacteria and soil colloid, while negative interaction energy indicates an attraction (Vigeant and Ford, 1997). As shown in Fig. 4, the total interaction energies remained positive (repulsive forces) for long separation distances (0–50 nm). The repulsive energy barriers (at separation distances = 1–2 nm) were greater than 100 kT. Pathogens could not overcome the sizable repulsions (Kim et al., 2010). Heights of the bacteria–colloid interaction energy barriers were in the following order: *E. coli* WH09 – NOM-present

Table 2 – Freundlich parameters for *S. suis* SC05 and *E. coli* WH09 adhesion to soil colloids at pH 6.0 and 1 mM KCl.

Soil type	*S. suis* SC05			*E. coli* WH09		
	K_f (mL g^{-1})	$1/n$	R^2	K_f (mL g^{-1})	$1/n$	R^2
NOM-present colloid	252.6	0.52	0.971	31.3	0.59	0.993
NOM-stripped colloid	856.1	0.60	0.991	210.6	0.68	0.979

The Freundlich equation is expressed as: $C_s = K_f \cdot C^{1/n}$, where K_f is the coefficient related to adhesion capacity, and $1/n$ is the linearity exponent.

colloid (228.3 kT) > *E. coli* WH09 – NOM-stripped colloid (162.9 kT) > *S. suis* SC05 – NOM-present colloid (139.5 kT) > *S. suis* SC05 – NOM-stripped colloid (101.1 kT). Thus, it is realistic to expect that the amount of adhesion was inversely correlated with the repulsive energy barrier heights. Indeed, the sequence of K_f values in Table 2 were in good agreement with the calculated energy barriers (Spearman correlation coefficient = −1.0, $P < 0.01$), indicating good agreement with the predictions of DLVO theory based on the sphere–sphere assumption.

The insert in Fig. 4 represents an enhanced view of the secondary energy minima existing at a greater separation distance (>100 nm). A secondary energy minimum emerges because the electrostatic repulsion decreases exponentially with the distance, while van der Waals attraction exhibits a slower decay (Tufenkji and Elimelech, 2004). Bacterial cells that were unable to overcome the sizable energy barriers likely are weakly and reversibly bound within the secondary energy minimum (about −0.02 kT), which was 101–107 nm away from the soil colloid surface (Redman et al., 2004; Syngouna and Chrysikopoulos, 2010). The attractive hydrophobic force is strong at separation distances below 10 nm and decays exponentially with distance (Israelachvili and Pashley, 1984; Meyer et al., 2006), thus the hydrophobic interaction is unlikely to be responsible for the overall interactions across these long distances (101–107 nm). The average kinetic energy of micron-sized particles is on the order of 1 kT, which is higher than the calculated energy minima (~0.02 kT) in this experiment (Tufenkji and Elimelech, 2004). Therefore, non-DLVO force such as polymer bridging attraction is likely contributing to the adhesion. Long polymer chains on bacterial and soil colloidal surfaces can bridge the gap between them and form covalent or hydrogen bonds, allowing for more stable cell adhesion at the secondary energy minimum (Grasso et al., 2002; Chen and Walker, 2007). Another two possible reasons are as follows: (1) additional kinetic energy (e.g., hydrodynamic shear force) from the rotating adhesion system in this study (150 rev min^{-1}) could help cells to approach the soil colloids and promote polymer bridging interaction (Hong et al., 2012). Li et al. (2000) and Thomas et al. (2002) also reported that bacterial (*Staphylococcus aureus* Phillips and *E. coli* F18) adhesion to surfaces (e.g., collagen, red blood cell) was enhanced by shear force in dynamic experimental systems; (2) soil surface charge heterogeneity affected adhesion processes. Brown soil colloids in this study mainly consisted of kaolinite, hydromica and vermiculite. Kaolinite is made of one silica tetrahedral sheet and one alumina octahedral sheet, while hydromica and vermiculite consist of one octahedral sheet sandwiched between two tetrahedral sheets (Cai et al., 2013). At pH 5.6–5.8, the plane and edge surfaces of alumina octahedral surface were positively charged (Sposito, 1984; Gupta et al., 2011), which may cause regions for favorable interactions and cell adhesion to soil surfaces via the reduction of electrostatic energy barriers (Walker et al., 2005b).

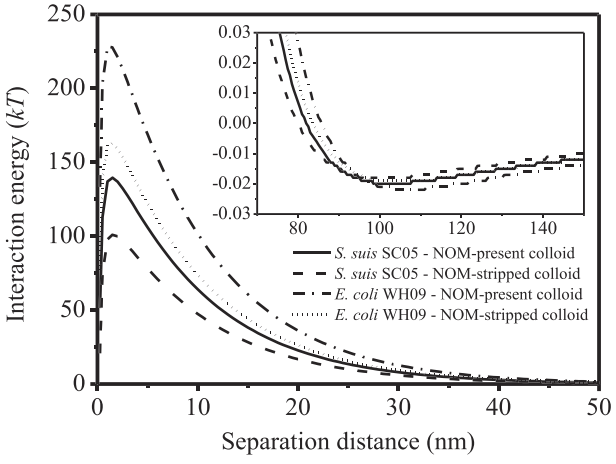

Fig. 4 – Interaction energy profiles between cells (*S. suis* SC05 and *E. coli* WH09) and soil colloids (NOM-present and NOM-stripped colloids) at pH 6.0 and 1 mM KCl as a function of separation distance. The figure insert highlights the corresponding secondary energy minima.

3.3. *Influence of pH*

The adhesion of *S. suis* SC05 and *E. coli* WH09 to soil colloids at varying pH is shown in Fig. 5. It was not surprising to find that more pathogens were adhered at the lowest pH 4.0. In general, bacterial adhesion decreased by 14.6–52.1% with increasing pH from 4.0 to 9.0. This phenomenon was consistent with the increased negative charges on the cell and soil colloid surfaces (Fig. 1a), causing greater electrostatic repulsive forces to exist at higher pH (Shashikala and Raichur, 2002; Zhao et al., 2012).

As observed in Table S1, the energy barriers were the lowest (0.5–144.5 kT) at pH 4.0, and the values generally increased with solution pH. Stronger repulsive interaction energies corresponded to fewer adhered cells (Fig. 6). These predictions from the DLVO theory agree well with the adhesion tendency. *S. suis* SC05 could overcome the minor energy barriers (0.5–1.3 kT) at pH 4.0 by shear force or Brownian motion under such near-favorable conditions (Haznedaroglu et al., 2009). However, the energy barriers (86.6–144.5 kT) were still too high for *E. coli* WH09 to form irreversible interaction at the same pH 4.0 (Hahn and O'Melia, 2004;

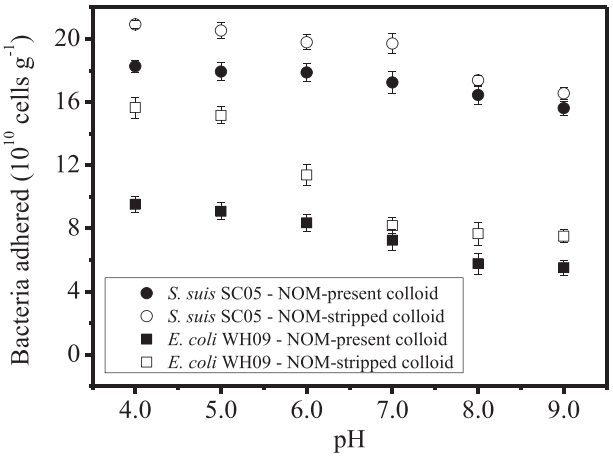

Fig. 5 – Effect of pH (4.0–9.0) on the adhesion of *S. suis* SC05 and *E. coli* WH09 to soil colloids (at 1 mM KCl). Error bars are the standard deviation of three replicates.

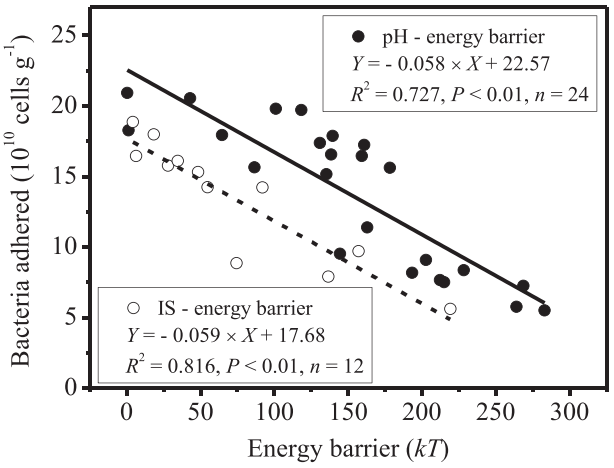

Fig. 6 – Bacterial adhesion amount (Y) correlated with energy barriers (X) at pH 4.0–9.0 and IS 1–100 mM. The solid and dashed lines stand for linear regression fits to the adhesion data at different pH and IS, respectively, which show significantly negative correlations ($P < 0.01$).

Haznedaroglu et al., 2009). The statistical relationship between adhesion amount and energy barrier was tested by linear regression (Fig. 6). It revealed that bacterial adhesion amount was negatively correlated with the energy barrier heights (linear correlation, $Y = -0.058\ X + 22.57$, $R^2 = 0.727$, $P < 0.01$), which clearly confirms the major role of DLVO-type forces over the pH range. However, cell adhesion amounts at varied pH were not positively correlated with the corresponding hydrophobicity values of pathogens or soil colloids (linear correlation, $P > 0.05$). The hydrophobic interaction could not explain the adhesion trends at long separation distances (49–110 nm, Table S1), which demonstrates its negligible role in the adhesion process.

When pH increased from 4.0 to 9.0, cell adhesion to NOM-stripped colloid and NOM-present colloid decreased by 20.9–52.1% and 14.6–42.2%, respectively. It is firstly reported in this paper that NOM-stripped colloid was observed to exhibit a higher decreasing rate of adhered cells with the increase of pH. Interestingly, the energy barriers of pathogen – NOM-stripped colloid system at pH 9.0 were 2.5–277.2 times as high as those at pH 4.0, which were also greater than the ratio of change (2.0–137.2 times) in energy barriers of pathogen – NOM-present colloid at different pH. This phenomenon was due to the different changing extent of negative charges on soil colloid surfaces. Fig. 1a shows that the rate of increase in negative charges on NOM-stripped colloid (49.7%) from pH 4.0 to 9.0 was higher than that on NOM-present colloid (23.0%), leading to the greater changes in the electrostatic repulsive forces between pathogens and NOM-stripped colloid. As is well known, pH-dependent variable charges in soil colloids are sensitive to solution pH (Uehara and Gillman, 1980; Qafoku et al., 2004) and responsible for the variance of zeta potential values. More variable charge sites on soil colloid surface (e.g., variable-charge mineral kaolinite in the examined soil colloid) were likely to be exposed after the coating NOM was removed (Wu et al., 2011). Hence, the higher amount of variable charges may contribute to the larger variation in bacterial adhesion to NOM-stripped colloid.

3.4. *Influence of ionic strength*

Fig. 7 illustrates the effect of IS on pathogen adhesion to soil colloids. The number of adhered cells increased by 15.9–89.2% with solution IS ranging from 1 mM to 50 mM ($P < 0.05$). According to the trends in zeta potential with IS as displayed in Fig. 1b, this increasing adhesion phenomenon qualitatively agrees with the expectations based on reduced electrostatic repulsion and double-layer thickness (Debye–Hückel length) with increasing IS. The calculated thickness values of electrical double layers decreased from 9.64 nm to 1.36 nm with the increase of IS from 1 mM to 50 mM (Fig. S2), leading to the weaker repulsive electrostatic interactions. The same adhesion trend was also observed in both batch and flow systems for other bacterial strains (Mills et al., 1994; Vigeant et al., 2002; Chen and Walker, 2012). Table S2 further verifies that increasing IS (1–50 mM) substantially lowered the energy barriers (219.3–4.3 kT, no energy barrier at IS 50 mM), which promoted cells adhesion to soil colloids. The secondary energy minimum depth (−0.020 to −0.513 kT) was deepened and its location approached the soil surface (107–15 nm) with increasing IS. The hydrophobicity of pathogens and soil colloids mostly displayed no significant difference ($P > 0.05$) at IS 1–10 mM or decreased ($P < 0.05$) at IS 10–50 mM for *E. coli* WH09 (Fig. 2b). Thus, the hydrophobic effect made no contribution to the increase in adhesion. As seen in Fig. 6, adhesion results were significantly correlated with energy barriers at low IS (1–10 mM) ($Y = -0.059\ X + 17.68$, $R^2 = 0.816$, $P < 0.01$), indicating that DLVO-type interactions had significant impacts on the adhesion behavior at low IS. Additionally, the influence of microscopic charge heterogeneities of soil colloids on pathogen adhesion may also be involved with the decreased values of double layer thicknesses and separation distances at IS 1–50 mM (Bradford and Kim, 2012). It has been reported that a larger number of colloids interacted with local

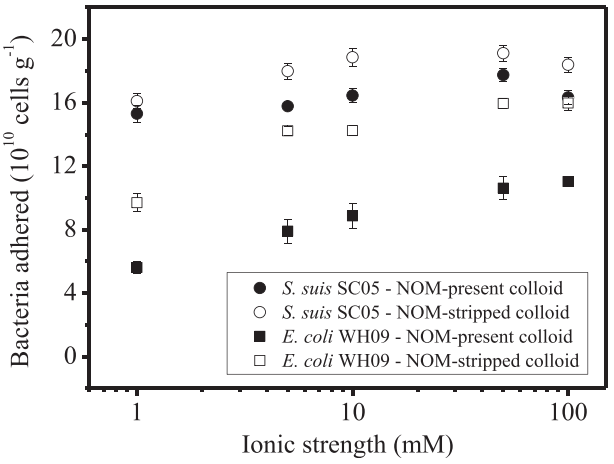

Fig. 7 – Effect of IS (1–100 mM) on the adhesion of *S. suis* SC05 and *E. coli* WH09 to soil colloids (at unadjusted pH of 5.6–5.8). Error bars are the standard deviation of three replicates.

positive sites (i.e., favorable patches) on sand at a thinner (higher IS) than a thicker (lower IS) double layer as they moved near the solid surface (Torkzaban et al., 2010). While increasing the solution IS (50–100 mM) continuously, the adhesion amount of *E. coli* WH09 to soil colloids was unchanged and reached a plateau ($P > 0.05$). This trend agrees well with the statistically unchanging zeta potentials of *E. coli* WH09 and soil colloids at IS 50–100 mM, suggesting the similar extent of electrostatic repulsion is expected. However, *S. suis* SC05 adhesion to soil colloids decreased slightly with increasing IS from 50 to 100 mM ($P < 0.05$), which deviated from the prediction of DLVO theory. The result demonstrates that DLVO forces alone are insufficient to quantitatively explain the adhesion mechanisms at higher IS 100 mM (Chen and Walker, 2007).

Table S2 suggests that no energy barrier or secondary energy minimum occurred at IS 100 mM (favorable interaction conditions). Total interaction forces were all attractive and *S. suis* SC05 cell was able to approach at smaller separation distances (<15 nm) than *E. coli* WH09 (<21 nm). Under this condition, short-range non-DLVO forces may be responsible for the decreasing adhesion trend of *S. suis* SC05 (Grasso et al., 2002; Chen and Walker, 2012). The hydrophobicities of *S. suis* SC05 decreased more sharply (by 9.0%) than those of *E. coli* WH09 (by 3.2%) from IS 50–100 mM (Fig. 2b). The greater reduction in short-range hydrophobic effect may inhibit *S. suis* SC05 adhesion at the closest separation distance of <15 nm, while the influence of hydrophobicity on *E. coli* WH09 adhesion was not obvious at a longer distance (<21 nm). It is well documented that the hydrophobic results among interacting surfaces are often contradictory (Meyer et al., 2006). For instance, Stenström (1989) observed a positive correlation between cell surface hydrophobicities (*Streptococcus faecalis*, *Streptococcus faecium*, *E. coli*, *Citrobacter freundii*, *Shigella sonnei*, and *Shigella boydii*) and their adhesion to mineral particles (quartz, albite, feldspar, and magnetite). Rochex et al. (2004) also found that attractive hydrophobic interactions were involved in *P. putida* adhesion to cellulose fibers, whereas Li and Logan (2004) reported the adhesion of bacteria (*E. coli*, *Pseudomonas aeruginosa*, *Burkholderia cepacia*, and *Bacillus subtilis*) to glass and metal-oxide surfaces was not significantly correlated with cell hydrophobicities. These contradictory results may have originated from the different interaction distances. However, the above research did not calculate the separation distances under a wide range of solution chemistry. In the current study, the extent of hydrophobic effect at pH 4.0–9.0 and IS 1–100 mM was found to be dependent on the separation distance predicted by the DLVO theory. Thus, it is tentatively concluded that both parameters of separation distance and hydrophobic value should be considered to effectively determine the hydrophobic interaction between bacteria and soils. Besides, additional experiments (e.g., atomic force microscopic measurements) are required to directly investigate the magnitude of hydrophobic effect as a function of separation distance.

On the other hand, polymer interaction may also contribute to the decreasing trend for *S. suis* SC05 at IS 100 mM. The EPS chains of bacteria were extended out from the cell surface into solution at lower IS, and could increase binding sites for polymer bridging between the pathogens and soil colloids (Grasso et al., 2002). However, the EPS chains became more rigid above a certain high IS (100 mM in this study) due to the large amounts of ions suspended among the polymers (Chen and Walker, 2007). This steric stabilization limited the approach distance of *S. suis* SC05 to soil colloid. Thereby, the occurring strong steric repulsion could overcome the electrostatic force and dominate the adhesion behavior at short distance (Abu-Lail and Camesano, 2003; Chen and Walker, 2007). The total EPS and protein contents of *S. suis* SC05 were 2.1–6.0 times as high as those of *E. coli* WH09 (Table 1), which possibly exhibited larger steric hindrance between the *S. suis* SC05 surface macromolecules and soil colloids.

It should be noted that the rate of decrease in *S. suis* SC05 adhesion to NOM-present colloid (by 8.0%) was larger than that to NOM-stripped colloid (by 3.8%). Previous works have shown colloidal or bacterial adhesion decreased in the presence of coated organic matter through increased steric repulsive forces (Bob and Walker, 2000; Mosley et al., 2003). The interaction of NOM on soil colloid with *S. suis* SC05 EPS chains could further enhance the steric repulsion. Thereby, it would be helpful to investigate the exact steric force values toward a better understanding of the polymer interaction mechanisms between pathogen and soil particles at the molecular level.

4. Conclusions

Pathogen adhesion to natural soil colloids over the pH range from 4.0 to 9.0 and at lower IS (≤50 mM) are governed by long-range DLVO forces, polymer bridging interactions and charge heterogeneity. At higher IS condition (100 mM), short-range steric repulsion and hydrophobic interaction play more important roles in *S. suis* SC05 adhesion at separation distances <15 nm. NOM in soil colloids significantly inhibits bacterial adhesion through increased surface charge, steric hindrance and screening of pH-dependent variable charge.

In soil environments, pathogens may be retained tightly in the upper layers of acidic and saline soils, therefore increasing their likelihood of crop contamination and mammal infection. Soil colloids of low NOM contents tend to associate preferentially with pathogens and facilitate bacterial long-distance transport in saturated soil systems. Additionally, pathogens that possess more negative surface charges and lower EPS contents are more likely to migrate through soil to water sources. The surface characteristics of both cells and soil particles must be considered when assessing adhesion processes. This work highlights the importance of comprehensively characterizing surface properties in order to effectively predict pathogen fate in natural soils.

Acknowledgments

This work was supported by the National Natural Science Foundation of China (41171196 and 40825002), Foundation for the Author of National Excellent Doctoral Dissertation of China (201066), Program for New Century Excellent Talents (NCET-11-0645) and the Fundamental Research Funds for the

Central Universities (2011PY005). The authors also acknowledge Professor Junlong Zhao from the State Key Laboratory of Agricultural Microbiology for providing the *S. suis* SC05 and *E. coli* WH09 isolates.

Appendix A. Supplementary data

Supplementary data related to this article can be found at http://dx.doi.org/10.1016/j.watres.2014.01.009

REFERENCES

Abu-Lail, N.I., Camesano, T.A., 2003. Role of ionic strength on the relationship of biopolymer conformation, DLVO contributions, and steric interactions to bioadhesion of *Pseudomonas putida* KT2442. Biomacromolecules 4, 1000–1012.

Alizadeh-Pasdar, N., Li-Chan, E.C., 2000. Comparison of protein surface hydrophobicity measured at various pH values using three different fluorescent probes. J. Agric. Food Chem. 48, 328–334.

Amirbahman, A., Olson, T.M., 1993. Transport of humic matter-coated hematite in packed beds. Environ. Sci. Technol. 27, 2807–2813.

Bakker, D.P., Postmus, B.R., Busscher, H.J., van der Mei, H.C., 2004. Bacterial strains isolated from different niches can exhibit different patterns of adhesion to substrata. Appl. Environ. Microbiol. 70, 3758–3760.

Bob, M.M., Walker, H.W., 2000. Effect of natural organic coatings on the polymer-induced coagulation of colloidal particles. Colloids Surf. Physicochem. Eng. Aspects 177, 215–222.

Bradford, M.M., 1976. A rapid and sensitive method for the quantitation of microgram quantities of protein utilizing the principle of protein-dye binding. Anal. Biochem. 72, 248–254.

Bradford, S.A., Kim, H.N., 2012. Causes and implications of colloid and microorganism retention hysteresis. J. Contam. Hydrol. 138–139, 83–92.

Brady, N.C., 1990. The Nature and Properties of Soils. Macmillan Publishing Company, New York.

Browner, C.M., Fox, J.C., Frace, S.E., Anderson, D.F., Goodwin, J., Shriner, P.H., 2001. Development Document for the Proposed Revisions to the National Pollutant Discharge Elimination System Regulation and the Effluent Guidelines for Concentrated Animal Feeding Operations. Engineering and Analysis Division, Office of Science and Technology, U.S. Environmental Protection Agency, Washington, DC.

Bruinsma, G.M., Rustema-Abbing, M., van der Mei, H.C., Busscher, H.J., 2001. Effects of cell surface damage on surface properties and adhesion of *Pseudomonas aeruginosa*. J. Microbiol. Methods 45, 95–101.

Cai, P., Huang, Q.Y., Zhang, X.W., 2006. Interactions of DNA with clay minerals and soil colloidal particles and protection against degradation by DNase. Environ. Sci. Technol. 40, 2971–2976.

Cai, P., Huang, Q.Y., Walker, S.L., 2013. Deposition and survival of *Escherichia coli* O157:H7 on clay minerals in a parallel plate flow system. Environ. Sci. Technol. 47, 1896–1903.

Cao, Y.Y., Wei, X., Cai, P., Huang, Q.Y., Rong, X.M., Liang, W., 2011. Preferential adsorption of extracellular polymeric substances from bacteria on clay minerals and iron oxide. Colloids Surf. B: Biointerfaces 83, 122–127.

Chen, G., Walker, S.L., 2007. Role of solution chemistry and ion valence on the adhesion kinetics of groundwater and marine bacteria. Langmuir 23, 7162–7169.

Chen, G., Walker, S.L., 2012. Fecal indicator bacteria transport and deposition in saturated and unsaturated porous media. Environ. Sci. Technol. 46, 8782–8790.

Cotruvo, J.A., Dufour, A., Rees, G., Bartram, J., Carr, R., Cliver, D.O., Craun, G.F., Fayer, R., Gannon, V.P.G., 2004. Waterborne Zoonoses – Identification, Causes and Control. IWA Publishing, London.

Deo, N., Natarajan, K.A., Somasundaran, P., 2001. Mechanisms of adhesion of *Paenibacillus polymyxa* onto hematite, corundum and quartz. Int. J. Mineral Process. 62, 27–39.

Dhand, N.K., Toribio, J.A., Whittington, R.J., 2009. Adsorption of *Mycobacterium avium* subsp. *paratuberculosis* to soil particles. Appl. Environ. Microbiol. 75, 5581–5585.

Elimelech, M., Nagai, M., Ko, C.H., Ryan, J.N., 2000. Relative insignificance of mineral grain zeta potential to colloid transport in geochemically heterogeneous porous media. Environ. Sci. Technol. 34, 2143–2148.

Fagbenro, J.A., Agboola, A.A., 1999. Effect of aerial oxidation pretreatment on composition and effectiveness of a Nigerian lignite sample as soil organic matter amendment. Commun. Soil. Sci. Plant Anal. 30, 2331–2344.

Farahat, M., Hirajima, T., Sasaki, K., 2010. Adhesion of *Ferroplasma acidiphilum* onto pyrite calculated from the extended DLVO theory using the van Oss-Good-Chaudhury approach. J. Colloid Interface Sci. 349, 594–601.

Foppen, J.W., Liem, Y., Schijven, J., 2008. Effect of humic acid on the attachment of *Escherichia coli* in columns of goethite-coated sand. Water Res. 42, 211–219.

Gordesli, F.P., Abu-Lail, N.I., 2012. Combined poisson and soft-particle DLVO analysis of the specific and nonspecific adhesion forces measured between *L. monocytogenes* grown at various temperatures and silicon nitride. Environ. Sci. Technol. 46, 10089–10098.

Gottschalk, M., Segura, M., Xu, J., 2007. *Streptococcus suis* infections in humans: the Chinese experience and the situation in North America. Anim. Health Res. Rev. 8, 29–46.

Gottschalk, M., Xu, J., Calzas, C., Segura, M., 2010. *Streptococcus suis*: a new emerging or an old neglected zoonotic pathogen? Future Microbiol. 5, 371–391.

Grasso, D., Subramaniam, K., Butkus, M., Strevett, K., Bergendahl, J., 2002. A review of non-DLVO interactions in environmental colloidal systems. Rev. Environ. Sci. Biotechnol. 1, 17–38.

Gregory, J., 1981. Approximate expressions for retarded van der Waals interaction. J. Colloid Interface Sci. 83, 138–145.

Guber, A.K., Pachepsky, Y.A., Shelton, D.R., Yu, O., 2007. Effect of bovine manure on fecal coliform attachment to soil and soil particles of different sizes. Appl. Environ. Microbiol. 73, 3363–3370.

Gupta, V., Hampton, M.A., Stokes, J.R., Nguyen, A.V., Miller, J.D., 2011. Particle interactions in kaolinite suspensions and corresponding aggregate structures. J. Colloid Interface Sci. 359, 95–103.

Hahn, M.W., O'Melia, C.R., 2004. Deposition and reentrainment of Brownian particles in porous media under unfavorable chemical conditions: some concepts and applications. Environ. Sci. Technol. 38, 210–220.

Haznedaroglu, B., Bolster, C., Walker, S., 2008. The role of starvation on *Escherichia coli* adhesion and transport in saturated porous media. Water Res. 42, 1547–1554.

Haznedaroglu, B.Z., Kim, H.N., Bradford, S.A., Walker, S.L., 2009. Relative transport behavior of *Escherichia coli* O157:H7 and *Salmonella enterica* Serovar Pullorum in packed bed column systems: influence of solution chemistry and cell concentration. Environ. Sci. Technol. 43, 1838–1844.

He, L.M., Tebo, B.M., 1998. Surface charge properties of and Cu (II) adsorption by spores of the marine *Bacillus* sp. strain SG-1. Appl. Environ. Microbiol. 64, 1123–1129.

Hiemenz, P.C., 1977. Electrophoresis and other electrokinetic phenomena. In: Lagowski, J.J. (Ed.), Principles of Colloid and Surface Chemistry. Marcel Dekker, New York, pp. 452–487.
Hogg, R., Healy, T., Fuerstenau, D., 1966. Mutual coagulation of colloidal dispersions. Trans. Faraday Soc. 62, 1638–1651.
Hong, Z.N., Rong, X.M., Cai, P., Dai, K., Liang, W., Chen, W.L., Huang, Q.Y., 2012. Initial adhesion of *Bacillus subtilis* on soil minerals as related to their surface properties. Eur. J. Soil. Sci. 63, 457–466.
Hong, Z.N., Zhao, G., Chen, W.L., Rong, X.M., Cai, P., Dai, K., Huang, Q.Y., 2013. Effects of solution chemistry on bacterial adhesion with phyllosilicates and goethite explained by the extended DLVO theory. Geomicrobiol. J.. http://dx.doi.org/10.1080/01490451.2013.824523.
Huang, G., Han, L., Yang, Z., Wang, X., 2008. Evaluation of the nutrient metal content in Chinese animal manure compost using near infrared spectroscopy (NIRS). Bioresour. Technol. 99, 8164–8169.
Israelachvili, J., Pashley, R., 1984. Measurement of the hydrophobic interaction between two hydrophobic surfaces in aqueous electrolyte solutions. J. Colloid Interface Sci. 98, 500–514.
Kim, H.N., Walker, S.L., 2009. *Escherichia coli* transport in porous media: influence of cell strain, solution chemistry, and temperature. Colloids Surf. B: Biointerfaces 71, 160–167.
Kim, H.N., Walker, S.L., Bradford, S.A., 2010. Macromolecule mediated transport and retention of *Escherichia coli* O157:H7 in saturated porous media. Water Res. 44, 1082–1093.
Kirby, B.J., Hasselbrink, E.F., 2004. Zeta potential of microfluidic substrates: 1. Theory, experimental techniques, and effects on separations. Electrophoresis 25, 187–202.
Li, B., Logan, B.E., 2004. Bacterial adhesion to glass and metal-oxide surfaces. Colloids Surfaces B: Biointerfaces 36, 81–90.
Li, Z.J., Mohamed, N., Ross, J.M., 2000. Shear stress affects the kinetics of *Staphylococcus aureus* adhesion to collagen. Biotechnol. Prog. 16, 1086–1090.
Meyer, E.E., Rosenberg, K.J., Israelachvili, J., 2006. Recent progress in understanding hydrophobic interactions. Proc. Natl. Acad. Sci. 103, 15739–15746.
Mills, A.L., Herman, J.S., Hornberger, G.M., DeJesús, T.H., 1994. Effect of solution ionic strength and iron coatings on mineral grains on the sorption of bacterial cells to quartz sand. Appl. Environ. Microbiol. 60, 3300–3306.
Morrow, J.B., Stratton, R., Yang, H.H., Smets, B.F., Grasso, D., 2005. Macro- and nanoscale observations of adhesive behavior for several *E. coli* strains (O157:H7 and environmental isolates) on mineral surfaces. Environ. Sci. Technol. 39, 6395–6404.
Mosley, L.M., Hunter, K.A., Ducker, W.A., 2003. Forces between colloid particles in natural waters. Environ. Sci. Technol. 37, 3303–3308.
Nikaido, H., 2003. Molecular basis of bacterial outer membrane permeability revisited. Microbiol. Mol. Biology Rev. 67, 593–656.
Oliver, D.M., Clegg, C.D., Heathwaite, A.L., Haygarth, P.M., 2007. Preferential attachment of *Escherichia coli* to different particle size fractions of an agricultural grassland soil. Water, Air, Soil. Pollut. 185, 369–375.
Omoike, A., Chorover, J., 2004. Spectroscopic study of extracellular polymeric substances from *Bacillus subtilis*: aqueous chemistry and adsorption effects. Biomacromolecules 5, 1219–1230.
Pachepsky, Y.A., Sadeghi, A., Bradford, S., Shelton, D., Guber, A., Dao, T., 2006. Transport and fate of manure-borne pathogens: modeling perspective. Agric. Water Manag. 86, 81–92.
Parent, M.E., Velegol, D., 2004. *E. coli* adhesion to silica in the presence of humic acid. Colloids Surfaces B: Biointerfaces 39, 45–51.
Park, S.J., Kim, S.B., 2009. Adhesion of *Escherichia coli* to iron-coated sand in the presence of humic acid: a column experiment. Water Environ. Res. 81, 125–130.
Qafoku, N.P., Ranst, E.V., Noble, A., Baert, G., 2004. Variable charge soils: their mineralogy, chemistry and management. Adv. Agronomy 84, 159–215.
Redman, J.A., Walker, S.L., Elimelech, M., 2004. Bacterial adhesion and transport in porous media: role of the secondary energy minimum. Environ. Sci. Technol. 38, 1777–1785.
Rochex, A., Lecouturier, D., Pezron, I., Lebeault, J.M., 2004. Adhesion of a *Pseudomonas putida* strain isolated from a paper machine to cellulose fibres. Appl. Microbiol. Biotechnol. 65, 727–733.
Rong, X.M., Huang, Q.Y., He, X.M., Chen, H., Cai, P., Liang, W., 2008. Interaction of *Pseudomonas putida* with kaolinite and montmorillonite: a combination study by equilibrium adsorption, ITC, SEM and FTIR. Colloids Surf. B: Biointerfaces 64, 49–55.
Salerno, M.B., Logan, B.E., Velegol, D., 2004. Importance of molecular details in predicting bacterial adhesion to hydrophobic surfaces. Langmuir 20, 10625–10629.
Santamaria, J., Toranzos, G.A., 2003. Enteric pathogens and soil: a short review. Int. Microbiol. 6, 5–9.
Schinner, T., Letzner, A., Liedtke, S., Castro, F.D., Eydelnant, I.A., Tufenkji, N., 2010. Transport of selected bacterial pathogens in agricultural soil and quartz sand. Water Res. 44, 1182–1192.
Sharma, M., Chang, Y., Yen, T., 1985. Reversible and irreversible surface charge modification of bacteria for facilitating transport through porous media. Colloids Surf. 16, 193–206.
Shashikala, A.R., Raichur, A.M., 2002. Role of interfacial phenomena in determining adsorption of *Bacillus polymyxa* onto hematite and quartz. Colloids Surf. B: Biointerfaces 24, 11–20.
Shephard, J.J., Savory, D.M., Bremer, P.J., McQuillan, A.J., 2010. Salt modulates bacterial hydrophobicity and charge properties influencing adhesion of *Pseudomonas aeruginosa* (PA01) in aqueous suspensions. Langmuir 26, 8659–8665.
Soupir, M.L., Mostaghimi, S., Dillaha, T., 2010. Attachment of *Escherichia coli* and enterococci to particles in runoff. J. Environ. Qual. 39, 1019–1027.
Sposito, G., 1984. The Surface Chemistry of Soils. Oxford University Press, New York.
Stenström, T.A., 1989. Bacterial hydrophobicity, an overall parameter for the measurement of adhesion potential to soil particles. Appl. Environ. Microbiol. 55, 142–147.
Syngouna, V.I., Chrysikopoulos, C.V., 2010. Interaction between viruses and clays in static and dynamic batch systems. Environ. Sci. Technol. 44, 4539–4544.
Tazehkand, S.S., Torkzaban, S., Bradford, S.A., Walker, S.L., 2008. Cell preparation methods influence *Escherichia coli* D21g surface chemistry and transport in saturated sand. J. Environ. Qual. 37, 2108–2115.
Thomas, W.E., Trintchina, E., Forero, M., Vogel, V., Sokurenko, E.V., 2002. Bacterial adhesion to target cells enhanced by shear force. Cell 109, 913–923.
Torkzaban, S., Kim, H.N., Simunek, J., Bradford, S.A., 2010. Hysteresis of colloid retention and release in saturated porous media during transients in solution chemistry. Environ. Sci. Technol. 44, 1662–1669.
Tufenkji, N., Elimelech, M., 2004. Deviation from the classical colloid filtration theory in the presence of repulsive DLVO interactions. Langmuir 20, 10818–10828.
Tyrrel, S., Quinton, J.N., 2003. Overland flow transport of pathogens from agricultural land receiving faecal wastes. J. Appl. Microbiol. 94, 87–93.
Uehara, G., Gillman, G.P., 1980. Charge characteristics of soils with variable and permanent charge minerals: I. Theory. Soil. Sci. Soc. Am. J. 44, 250–252.
Unc, A., Goss, M.J., 2004. Transport of bacteria from manure and protection of water resources. Appl. Soil. Ecol. 25, 1–18.
Vigeant, M., Ford, R.M., 1997. Interactions between motile *Escherichia coli* and glass in media with various ionic strengths,

as observed with a three-dimensional-tracking microscope. Appl. Environ. Microbiol. 63, 3474–3479.
Vigeant, M.A.S., Ford, R.M., Wagner, M., Tamm, L.K., 2002. Reversible and irreversible adhesion of motile *Escherichia coli* cells analyzed by total internal reflection aqueous fluorescence microscopy. Appl. Environ. Microbiol. 68, 2794–2801.
Walker, S.L., Hill, J.E., Redman, J.A., Elimelech, M., 2005a. Influence of growth phase on adhesion kinetics of *Escherichia coli* D21g. Appl. Environ. Microbiol. 71, 3093–3099.
Walker, S.L., Redman, J.A., Elimelech, M., 2004. Role of cell surface lipopolysaccharides in *Escherichia coli* K12 adhesion and transport. Langmuir 20, 7736–7746.
Walker, S.L., Redman, J.A., Elimelech, M., 2005b. Influence of growth phase on bacterial deposition: interaction mechanisms in packed-bed column and radial stagnation point flow systems. Environ. Sci. Technol. 39, 6405–6411.
Wang, L., Xu, S., Li, J., 2011. Effects of phosphate on the transport of *Escherichia coli* O157:H7 in saturated quartz sand. Environ. Sci. Technol. 45, 9566–9573.
Wu, H.Y., Jiang, D.H., Cai, P., Rong, X.M., Dai, K., Liang, W., Huang, Q.Y., 2011. Adsorption of *Pseudomonas putida* on soil particle size fractions: effects of solution chemistry and organic matter. J. Soils Sediments 12, 143–149.
Xiong, Y., 1985. Soil Colloids, vol. 2. Science Press, Beijing.
Yee, N., Fein, J.B., Daughney, C.J., 2000. Experimental study of the pH, ionic strength, and reversibility behavior of bacteria-mineral adsorption. Geochim. Cosmochim. Acta 64, 609–617.
Zhao, W.Q., Liu, X., Huang, Q.Y., Walker, S.L., Cai, P., 2012. Interactions of pathogens *Escherichia coli* and *Streptococcus suis* with clay minerals. Appl. Clay Sci. 69, 37–42.
Zita, A., Hermansson, M., 1994. Effects of ionic strength on bacterial adhesion and stability of flocs in a wastewater activated sludge system. Appl. Environ. Microbiol. 60, 3041–3048.